

Hybrid-Functional Calculations of the Copper Impurity in Silicon

Abhishek Sharan,* Zhigang Gui, and Anderson Janotti

Department of Physics and Astronomy, University of Delaware, Newark, Delaware 19716, USA

*Department of Materials Science and Engineering, University of Delaware,
Newark, Delaware 19716, USA*

(Received 4 August 2016; revised manuscript received 7 July 2017; published 25 August 2017)

We calculate formation energies and transition levels for copper-related defects in silicon using the screened hybrid functional of Heyd, Scuseria, and Ernzerhof HSE06. We consider Cu sitting on interstitial sites (Cu_i), a substitutional site (Cu_{Si}), a $\text{Cu}_{\text{Si}}\text{-Cu}_i$ pair, a complex formed from substitutional Cu and interstitial hydrogen ($\text{Cu}_{\text{Si}}\text{-H}_i$), and a complex formed from a substitutional Cu and three interstitial Cu atoms ($\text{Cu}_{\text{Si}}\text{-3Cu}_i$). We find that Cu_i is a fast diffuser, with a migration barrier of only 0.19 eV, in good agreement with experimental values. Cu_i is a shallow donor and its formation energy is lower than that of Cu_{Si} for all Fermi-level positions in the band gap. Cu_{Si} , on the other hand, induces levels in the gap which are related to the occupation of antibonding states originating from the coupling between the Cu 3d states ($t_2^{(d)}$), resonant in the valence band, and the vacancy-induced gap states ($t_2^{(p)}$). The stable charge states of Cu_{Si} in the gap are +1, 0, -1, and -2. The transition levels of $\text{Cu}_{\text{Si}}\text{-Cu}_i$ and $\text{Cu}_{\text{Si}}\text{-H}_i$ are closely related to the levels of isolated Cu_{Si} : a donor level (+/0) near the valence band, an acceptor level near midgap, and a double-acceptor level in the upper part of the gap. The calculated transition levels are in good agreement with experimental results, and the formation energies explain the observed solubility.

DOI: 10.1103/PhysRevApplied.8.024023

I. INTRODUCTION

Copper is a common impurity in silicon, often present in the processing environment of Si wafers [1]. It has long been known that the presence of Cu in a Si-based p - n junction leads to an increase in leakage current [2–5]. It has also been reported that Cu may cause a breakdown in gate silicon oxide [6,7], resulting in leakage current in MOS capacitors. With the use of copper as interconnect material in integrated circuits [8], Cu contamination has become a major concern due to its detrimental effects on device operation. Copper is also considered for replacing silver for the front metallization of solar cells, potentially leading to cost reduction. Davis and co-workers [9,10] conducted the first systematic studies of the effect of Cu contamination on the minority carrier lifetime in Si, and the impact on solar-cell performance. The authors found that Cu concentrations up to 10^{16} cm^{-3} in Si had no effect on solar-cell efficiency. However, studies by other groups have shown a weak effect of low Cu contamination levels on minority-carrier lifetime in p -type [11–14] and a stronger effect on n -type silicon [12,15].

The behavior of Cu in Si has been considered extensively by experimentalists [16–42] as well as by theoreticians [43–55]. For a long time, the Cu concentration that was detrimental to device performance was uncertain, and reliable techniques for measuring the Cu contamination level was unavailable [19]. Studies performed by various groups in the last 30 yr have led to a better understanding of

the behavior of the Cu impurity and its impact on electrical and optical properties of Si crystals. Despite tremendous progress, there still remains marked disagreement between the theoretical and experimental results (see Fig. 1). While the geometries of interstitial and substitutional Cu point defects and complexes are relatively well understood, accurate predictions of transition levels with respect to the band edges, the absolute formation energies, and the solubilities are still lacking. Thus far, computational studies based on density-functional theory (DFT) have led only to a qualitative description.

Copper is a very fast diffuser in Si and tends to form complexes or precipitates [19,29]. Experiments indicate that, at high temperatures, almost all Cu is dissolved interstitially (Cu_i) under electronically intrinsic conditions. Only a small fraction of Cu atoms occupy substitutional sites, Cu_{Si} , typically less than 0.1% of the equilibrium concentration [18,19,35]. The solubility of Cu in Si reaches a maximum of $1.5 \times 10^{18} \text{ cm}^{-3}$ at 1300 °C [19]. From measurements of the Fermi-level dependence of equilibrium solubility and resistivity [18], it was concluded that interstitial Cu exists in the positive charge state; i.e., it acts as a single donor, Cu_i^+ , at all investigated temperatures. Early experiments on Cu diffusivity in p -type Si gave an effective migration barrier of 0.43 eV. This result was later reinterpreted and attributed to the effect of trapping of Cu_i^+ by acceptor impurities [24]. Experiments based on the transient-ion-drift technique indicate that Cu diffuses through a direct interstitial mechanism, with a migration barrier of 0.18 eV in electronically intrinsic conditions and moderately n -type doped material [24,37].

*asharan@udel.edu

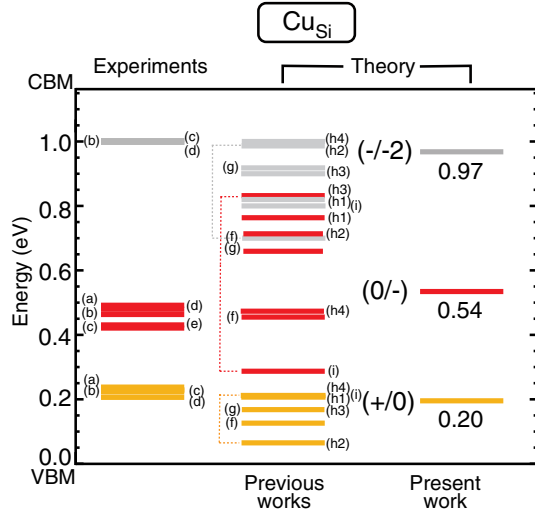


FIG. 1. Thermodynamic transition levels for the substitutional copper impurity in silicon (Cu_{Si}). The zero in energy is placed at the valence-band maximum (VBM). Experimental values are taken from (a) Ref. [17], (b) Ref. [21], (c) Ref. [22], (d) Refs. [30,33], and (e) Ref. [40]. The results from previous calculations [(f) Ref. [47], (g) Ref. [50], (h1–h4) Ref. [52], and (i) Ref. [55]] illustrate the wide spread in the theoretical values.

This very high diffusivity, i.e., approximately $2.4 \times 10^7 \text{ cm}^2/\text{s}$ at room temperature [37], suggests that an isolated Cu interstitial is rather unstable. Therefore, following high-temperature processing, the diffusivity of interstitial Cu at room temperature is still high enough that Cu_i either diffuses out of the material or forms complexes and precipitates, leaving only occupied substitutional sites as Cu-related point defects. Substitutional copper, Cu_{Si} , has been observed by an emission-channeling technique where the angular distribution of β^- particles emitted by the implanted radioactive isotope ^{67}Cu ions was monitored following annealing up to 600 °C [31,32]. It was reported that, after high-temperature annealing, all Cu atoms that occupy a near-substitutional site after implantation are converted to ideal substitutional lattice sites [32].

The impact of Cu impurities on the electrical properties of bulk Si has been widely reported in the literature, with both experimental and theoretical results, yet there still exists marked disagreement on the position of the transition levels with respect to the band edges. Deep-level-transient-spectroscopy (DLTS) experiments reveal a donor level 0.15 eV below the conduction band, which has been attributed to either isolated Cu_i or a Cu_i -related complex [23]. This conclusion contrasts with DFT calculations which indicate that Cu_i is a hydrogenic shallow donor [50,51].

Transition levels associated with substitutional copper are difficult to extract due to the low concentrations of isolated Cu_{Si} under equilibrium conditions [25]. Experiments suggest that Cu_{Si} displays an amphoteric behavior, with acceptor and donor levels in the band gap

[17,21,22,30,33,40]. Early results of temperature-dependent Hall measurements revealed two levels, one at 0.24 and another at 0.49 eV above the valence band, which were attributed to the donor (+/0) and acceptor (0/−) levels of Cu_{Si} [17]. Early DLTS measurements also detected two levels, at 0.23 and 0.43 eV above the valence band, that were assigned to the single donor and acceptor levels of Cu_{Si} [21,22]. A third level at 0.16 eV below the conduction band was correlated with the two other levels and accordingly assigned to the (−/−2) double-acceptor level of Cu_{Si} [21,22]. Later, DLTS experiments performed by another group observed levels at 0.207 and 0.478 eV above the valence band, which were also assigned to the donor (+/0) and acceptor (0/−) levels of Cu_{Si} , and a third level at 0.167 eV below the conduction band, assigned to the double-acceptor (−/−2) level of Cu_{Si} [30,33]. More recently, Laplace-transform DLTS measurements give the (+/0) level at 0.225 eV and the (0/−) level at 0.430 eV above the valence band [40]. A triple-acceptor level (−2/−3) related to Cu_{Si} , as predicted by an analysis based on Hall measurements [18], has not been observed with DLTS.

While the experimental data for the transition levels lie in a relatively narrow range, the calculated transition levels for Cu_{Si} are spread in a too wide of an energy range [47,50,52,55], as shown in the center of Fig. 1. For instance, the reported values for the acceptor (0/−) level of Cu_{Si} vary in the range of 0.5 eV, which is about half of the band gap of crystalline Si. The main problem with existing reports on Cu impurity in Si based on DFT calculations is the band-gap error [56,57]. DFT within the local-density or generalized-gradient approximations (LDAs and GGAs) severely underestimate band gaps, leading to large errors in the position of transition levels with respect to the band edges [58]. Here, we revisit the problem of Cu-related defects in bulk Si using calculations based on a hybrid functional. We use the Heyd, Scuseria, and Ernzerhof hybrid functional HSE06 [59,60], which was shown to provide an accurate description of the Si electronic band structure, and it has been successful in predicting defect-induced levels in other semiconductor materials [61,62].

In the following, we describe the computational methods employed in this work, then present the results of formation energies and transition levels for isolated Cu_i and Cu_{Si} , and for the complexes $\text{Cu}_{\text{Si}}\text{-Cu}_i$, $\text{Cu}_{\text{Si}}\text{-H}_i$, and $\text{Cu}_{\text{Si}}\text{-3Cu}_i$. We examine our results in light of previous DFT calculations and experiments, and we discuss implications to Si-based electronic devices and solar cells.

II. COMPUTATIONAL APPROACH

Our calculations are based on the generalized Kohn-Sham theory [57,63,64] with the HSE06 hybrid functional [59,60] as implemented in the Vienna *ab initio* simulation package code [65,66]. In the HSE06 hybrid functional, the

exchange potential is separated into long-range and short-range parts. We use the standard screening parameter of the HSE06 hybrid functional, which is $\omega = 0.2$, where ω is related to the characteristic distance, $2/\omega$, which defines the range separation. In the short-range part, 25% of the nonlocal Hartree-Fock exchange is mixed with 75% of the semilocal exchange in the generalized-gradient approximation form of Perdew, Burke, and Ernzerhof (PBE) [67]. The correlation potential and the long-range part of the exchange are described by PBE. The interactions between the valence electrons and the ionic cores are treated using the projector-augmented-wave potentials [68,69].

The calculated equilibrium lattice parameter of Si is 5.433 Å, in good agreement with the experimental value of 5.4304 Å [70]. This calculation is performed using a primitive cell with two atoms, a $6 \times 6 \times 6$ mesh of special k points for integrations over the Brillouin zone, and a plane-wave cutoff of 369 eV. The electronic band structure is shown in Fig. 2. The calculated band gap is 1.16 eV, which is only slightly smaller than the low-temperature value of 1.17 eV [71]; the valence-band maximum (VBM) occurs at Γ and the conduction-band minimum (CBM) occurs along the Γ -X direction, near the X point.

The Cu impurity in Si is simulated by using a 64-atom supercell, which is a $2 \times 2 \times 2$ repetition of the eight-atom cubic unit cell. The integrations over the Brillouin zone are performed using a $2 \times 2 \times 2$ special k -point mesh. The effects of spin polarization are included. Tests performed using a supercell with 216 atoms ($3 \times 3 \times 3$ repetition of the eight-atom cubic unit cell) and $(1/4, 1/4, 1/4)$ as the special k point show that formation energies are converged to better than 0.1 eV. The stability of the impurity in a given configuration, i.e., substitutional and interstitial, is given by its formation energy, which depends on the Fermi-level position ε_F in the case of charged centers. For example, the formation energy of substitutional Cu in a given charge state q (Cu_{Si}^q) is determined by [72]

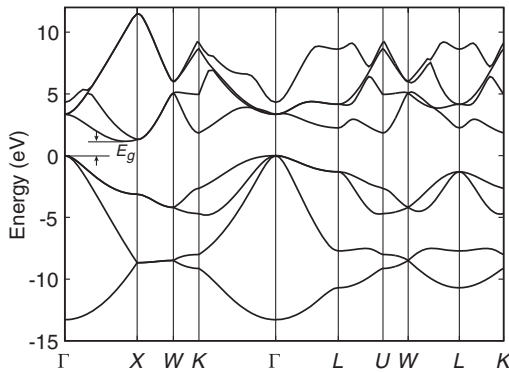


FIG. 2. Band structure of Si calculated using the HSE06 hybrid functional. The zero in energy is placed at the VBM, at the Γ point.

$$E^f(\text{Cu}_{\text{Si}}^q) = E_t(\text{Cu}_{\text{Si}}^q) - E_t(\text{Si}) + \mu_{\text{Si}} - \mu_{\text{Cu}} + q\varepsilon_F + \Delta^q, \quad (1)$$

where $E_t(\text{Cu}_{\text{Si}}^q)$ is the total energy of the supercell containing a Cu_{Si} in charge state q , and $E_t(\text{Si})$ is the total energy of a perfect Si crystal in the same supercell. The Si atom that is removed from the crystal is placed in a reservoir of energy μ_{Si} , which we take as the energy per atom of Si bulk. Similarly, the Cu atom that is added to the system is brought from a reservoir with energy μ_{Cu} , which is taken as the energy per atom of Cu bulk. The Fermi level ε_F is referenced to the VBM of the perfect crystal. Finally, the term Δ^q is a charge-state-dependent correction due to the finite size of the supercell [72].

The value of the Fermi level where the formation energy for the defect in charge state q equals that of the same defect in charge state q' defines the thermodynamic transition level (q/q') , which can be directly compared with levels obtained in DLTS and temperature-dependent Hall measurements. The thermodynamic transition level (q/q') can be computed using

$$(q/q') = \frac{E^f(\text{Cu}_{\text{Si}}^q; \varepsilon_F = 0) - E^f(\text{Cu}_{\text{Si}}^{q'}; \varepsilon_F = 0)}{q' - q}, \quad (2)$$

where $E^f(\text{Cu}_{\text{Si}}^q; \varepsilon_F = 0)$ is the formation energy of Cu_{Si} in the charge state q when the Fermi level is at the VBM ($\varepsilon_F = 0$). The concentration of the impurity in the dilute limit is determined by its formation energy:

$$c = N_0 \times e^{\frac{-E^f}{kT}}, \quad (3)$$

where N_0 is the number of sites per volume that the impurity can be incorporated on, k is the Boltzmann constant, and T the temperature. For the substitutional site in Si, $N_0 = 6.6 \times 10^{22} \text{ cm}^{-3}$.

III. RESULTS AND DISCUSSION

Different models for the electronic structure of the Cu impurity in silicon have been proposed over the years, from simple ionic models [73] to those based on self-consistent Hartree-Fock [46,48] and DFT calculations [44,47,50,53–55]. The ionic model for the substitutional Cu in bulk Si assumed that the 3d states are in the band gap [73], similar to the case of 3d transition-metal impurities in many oxides, and inferred that their occupation gives rise to observed levels in the gap. By contrast, another model suggested that the 3d states are inert and lie well below the bottom of the valence band [74–77]. Electronic-structure calculations based on DFT, however, reveal that the Cu d states are actually resonant in the valence band, and that the Cu_{Si} -related states that appear in the gap are ligand states [44,47]. As discussed below, we also find that the Cu d

states are resonant in the valence band for both interstitial and substitutional configurations.

We investigate five Cu-related defects: isolated interstitial (Cu_i), substitutional (Cu_{Si}), a $\text{Cu}_{\text{Si}}\text{-Cu}_i$ pair, a complex involving substitutional Cu and interstitial hydrogen ($\text{Cu}_{\text{Si}}\text{-H}_i$), and a complex involving substitutional Cu and three interstitial Cu atoms in the neighboring sites of substitutional Cu ($\text{Cu}_{\text{Si}}\text{-3Cu}_i$). The calculated formation energies as a function of the Fermi level are shown in Fig. 3. The isolated interstitial Cu_i behaves as a shallow donor, whereas the defects Cu_{Si} , $\text{Cu}_{\text{Si}}\text{-Cu}_i$, and $\text{Cu}_{\text{Si}}\text{-H}_i$ display amphoteric behavior, with a single-donor (+/0) level near the valence band, a single-acceptor level (0/-) near midgap, and a double-acceptor level (-/-2) in the upper part of the gap, closer to the conduction band. The complex $\text{Cu}_{\text{Si}}\text{-3Cu}_i$ induces a donor (+/0) and a double-donor level (+/+2) in the lower part of the gap. We note

that none of the Cu_{Si} -related defects exhibit a triple-acceptor level (-2/-3) in the band gap, contrary to an earlier suggestion based on solubility and diffusivity experiments [18] and DFT calculations using the Green's function [47].

A. Interstitial copper Cu_i

There are two high-symmetry interstitial sites in the Si crystal that can accommodate the Cu impurity, the tetrahedral and hexagonal interstitial sites. The tetrahedral site has four equally distanced Si nearest neighbors, while the hexagonal interstitial site has six Si nearest neighbors. The hexagonal site is located at the midpoint between two neighboring tetrahedral interstitial sites along the $\langle 111 \rangle$ direction. The local lattice geometry of Cu_i at the tetrahedral site is shown in Fig. 4(a).

We find that Cu_i is a shallow donor and contributes one electron to the conduction band, at either the tetrahedral or the hexagonal interstitial site. Cu_i is most stable at the tetrahedral interstitial site, and the hexagonal site is only 0.16 eV higher in energy. We calculate the migration barrier of Cu_i^+ using the nudged-elastic-band method within the HSE06 method. The results are shown in Fig. 4(d). The maximum energy in the migration path occurs at the point where the Cu_i passes through the plane formed by three Si nearest neighbors; the hexagonal is, therefore, a metastable configuration. The calculated migration barrier of 0.19 eV from Fig. 4(d) is in good agreement with the accepted value of 0.18 ± 0.02 eV based on measurements using the transient-ion-drift technique [24].

For comparison, we also perform calculations using the nudged-elastic-band method with the DFT GGA, which gives 0.11 eV as the migration barrier, and we find that the hexagonal interstitial site is the saddle point in the migration of Cu_i from one tetrahedral site to another. Previous calculations [54,78] also find that Cu at the hexagonal interstitial site is unstable and represents a maximum in the migration path of Cu_i ; however, the earlier report, based on the Hartree-Fock method, gives a barrier of 0.24 eV [78]. Previous calculations based on the DFT LDA or GGA give a barrier of 0.11 eV [54], which is consistent with our DFT-GGA results.

Our calculations show that Cu_i does not induce any levels in the gap, being stable only in the singly positive charge state, Cu_i^+ , for all Fermi-level positions in the band gap. This result is in agreement with previous DFT calculations [47,50], and it cannot explain previous assignment of a donor level at 0.15 eV below the conduction band to Cu_i [23]. In fact, we find that Cu_i is an effective-mass shallow donor; i.e., in the neutral charge state Cu_i^0 , the electron bound to the Cu impurity occupies a conduction-band-like state, with a typical donor ionization energy of tens of meV. This neutral charge state, Cu_i^0 , cannot be accurately described by our finite-size supercell calculations. We note that the neutral and -1 charge states and the

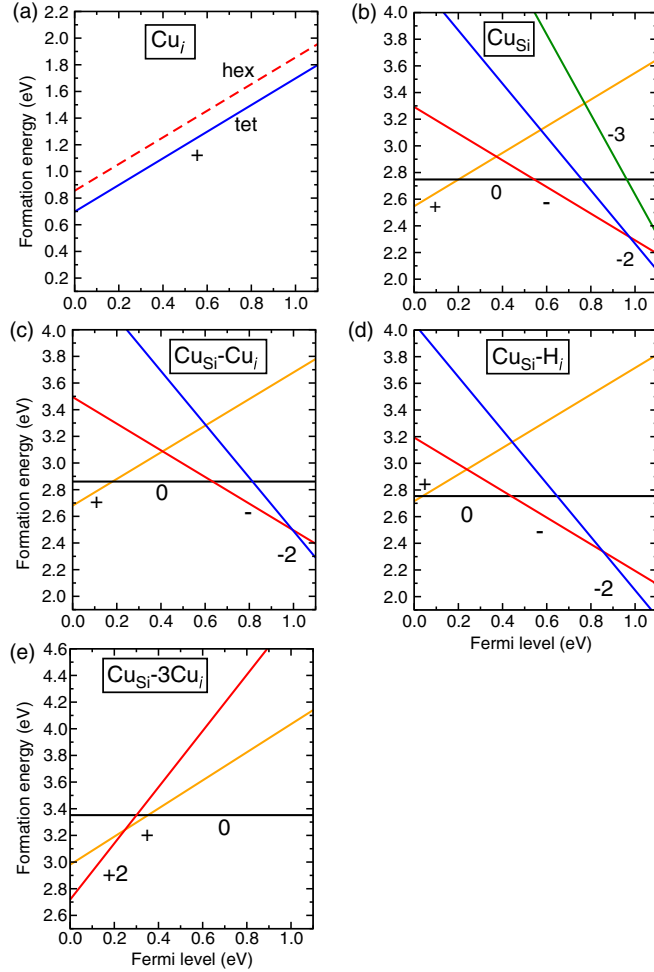


FIG. 3. Calculated formation energies as a function of Fermi level ϵ_F for copper-related defects in Si: (a) an isolated interstitial Cu_i at the tetrahedral (tet) and the hexagonal (hex) site, (b) substitutional Cu_{Si} , (c) a $\text{Cu}_{\text{Si}}\text{-Cu}_i$ pair, (d) a copper-hydrogen $\text{Cu}_{\text{Si}}\text{-H}_i$ complex, and (e) a $\text{Cu}_{\text{Si}}\text{-3Cu}_i$ complex. The zero in the Fermi level corresponds to the VBM at Γ .

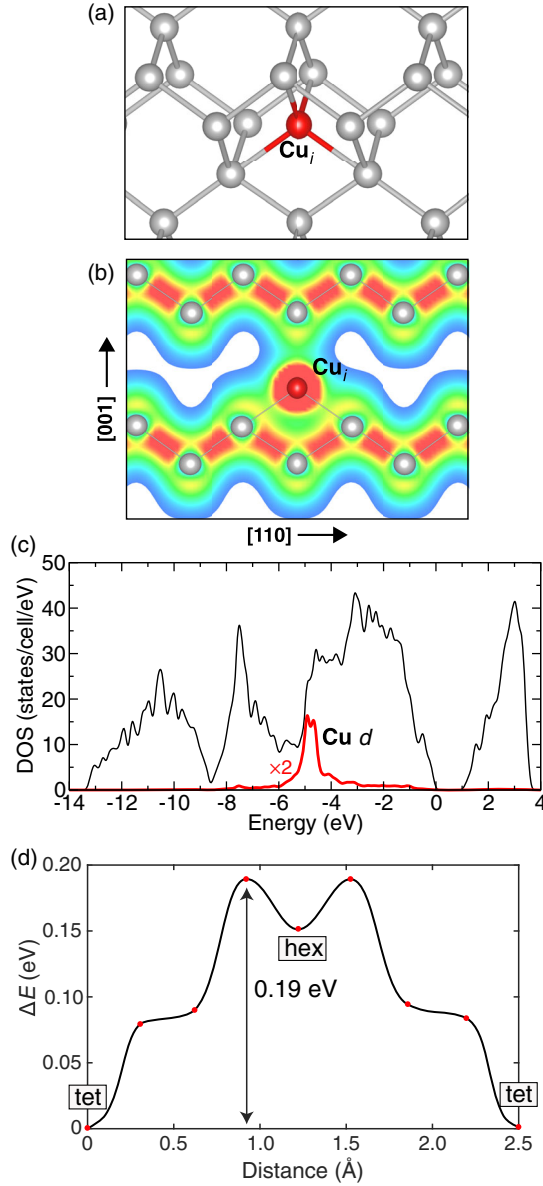


FIG. 4. (a) Ball-and-stick model of the local lattice structure of interstitial Cu at the tetrahedral site in the positive charge state (Cu_i^+). (b) Isosurfaces of the total valence charge distribution of Cu_i^+ in a (110) plane containing the Cu impurity and two nearest-neighbor Si atoms. (c) Total density of states (DOS) of a supercell containing Cu_i^+ and the projection on the Cu site showing the 3d contribution. (d) Migration energy barrier of Cu_i^+ from one tetragonal site (tet) and an equivalent site, passing through a hexagonal site (hex).

(+/-0), (0/+), and (0/-) levels in the gap assigned to Cu_i in previous work [54] are likely artifacts of the calculations due to the DFT-LDA or -GGA band-gap error; the added electrons for the neutral and -1 charge states probably occupy conduction-band-like states.

Cu_i^+ at the tetrahedral site forms four Cu—Si bonds of equal length that are 3.2% larger than the equilibrium Si—Si bond length. In Fig. 4(b), we show isosurfaces of the total

valence charge distribution in the (110) plane containing Cu_i^+ and one of its four Si nearest neighbors. We can see only a slight directional component of the Cu_i^+ —Si bond, indicating that the Cu_i^+ bond to Si host atoms has a strong ionic character. In Fig. 4(c), we show the total density of states of the supercell containing Cu_i^+ and the DOS projected on the Cu 3d orbital. The Cu 3d-related states appear at about 5 eV below the VBM. The two-peak structure is related to the $3d\ t_2^{(d)}$ and $e^{(d)}$ states that are split due to the crystal field, and the width indicates the strength of the coupling with the host states.

The formation energy of Cu_i^+ , shown in Fig. 3(a), is lower than that of the other Cu-related defects studied here—for all Fermi-level positions in the band gap—indicating that Cu is incorporated primarily into the interstitial sites under equilibrium conditions. The calculated formation energy explains the observed solubility of $1.5 \times 10^{18} \text{ cm}^{-3}$ at 1300 °C for Cu in Si [19]. At such a high temperature, the intrinsic carrier concentration is expected to dominate, placing the Fermi level near midgap. The experimental solubility follows an Arrhenius curve with a formation energy of 1.49 eV [19], suggesting that the Fermi level is located at 0.8 eV above the VBM, according to Fig. 3(a). Our results for the variation of the formation energy with the Fermi level in the case of Cu_i^+ , the relatively high formation energy even in *p*-type Si, and the calculated migration barrier of 0.19 eV explains the instability of isolated interstitial Cu in Si and, thus, its tendency to form complexes or precipitates. The present results are in much better agreement with experiments than previous calculations [54], which reported a formation energy of 1.99 eV. There are two main issues with these previous results: First, the formation energy is provided for the neutral charge state, where an electron is actually occupying a conduction-band-like state. Second, the position of the conduction band with respect to the valence band is severely underestimated due to the band-gap error in the DFT LDA or GGA. Although these two effects tend to cancel each other out, their results are still too far from the experimental value.

B. Substitutional copper Cu_{Si}

The calculated formation energy of Cu_{Si} is shown in Fig. 3(b), where we identify three transition levels in the band gap (on the right in Fig. 1). We find a donor level (+/0) at 0.20 eV, an acceptor level (0/-) at 0.54 eV, and a double-acceptor level (-/-2) at 0.97 eV above the valence band. A triple-acceptor level (-2/-3) is resonant in the conduction band, well above the CBM. Thus, we find that Cu_{Si} is amphoteric. In *p*-type Si, Cu_{Si} is most stable in the +1 charge state, acting as a compensation center, counteracting the hole conductivity. For a Fermi level lying between 0.20 and 0.54 eV, Cu_{Si} is stable in the neutral charge state and is, therefore, electrically inactive. For a

Fermi level between 0.54 and 0.97 eV, Cu_{Si} is stable in the -1 acceptor charge state. In n -type Si, i.e., for a Fermi-level position at or near the CBM, Cu_{Si} is most stable in the -2 charge state, acting as a compensation center for n -type conductivity. These results agree with previous DFT calculations [47,50,55], except that we find that the triple-acceptor charge state, $\text{Cu}_{\text{Si}}^{-3}$, is unstable; i.e., it occurs well above the CBM. This finding is in contrast to early DFT calculations [47] and a previous experimental report [18]. We note that the position of the transition levels with respect to the VBM reported in Ref. [55] are underestimated, likely due to the band-gap error that is typical in the DFT-LDA or -GGA method.

The transition levels of Cu_{Si} , reported above, are directly related to the impurity-induced gap states and their occupation, which are, in turn, a result of the chemical bonds that the impurity makes with the host atoms. For substitutional Cu in Si, we find two sets of impurity-induced states. One set is composed of three states (which can hold up to six electrons, with up and down spins) located in the band-gap region, while a second is composed of six fully occupied states (holding a total of 12 electrons) that are resonant in the valence band. These states have strong contributions from the impurity and the four nearest-neighbor Si atoms. In the neutral charge state, the gap states are occupied by three electrons; i.e., the gap states have three holes. The other possible charge states can be formed by removing one electron (Cu_{Si}^+) or adding one, two, or three electrons to form Cu_{Si}^- , $\text{Cu}_{\text{Si}}^{2-}$, and $\text{Cu}_{\text{Si}}^{3-}$, respectively. From the atom-projected density of states shown in Fig. 5(c), we note that the gap states have large contributions from the four Si nearest neighbors and, to a much lesser extent, from the Cu impurity. The states resonant in the valence band can be subdivided into three sets. A fully symmetric a_1 state, with large contributions from the Si nearest neighbors, a twofold-degenerate e state, and a lower threefold-degenerate t_2 state derived mostly from the Cu 3d orbitals.

The model that emerges from these results is depicted in Fig. 6. The Cu 3d states are resonant in the valence band and are split into t_2 and e (labeled $t_2^{(d)}$ and $e^{(d)}$) due to the crystal field. The $t_2^{(d)}$ states couple with the t_2 states composed of dangling bonds of the four Si nearest neighbors ($t_2^{(p)}$), pushing the latter to higher energies in the band gap. The $e^{(d)}$ states weakly interact with the host orbitals, while the a_1 state is a fully symmetric combination of the neighboring dangling bonds that couples weakly to the impurity 3d states. In the case of Cu_{Si}^0 , the $t_2^{(p)}$ gap states are partially occupied with three electrons (three holes).

By adding three electrons, i.e., forming $\text{Cu}_{\text{Si}}^{3-}$, the $t_2^{(p)}$ gap states are fully occupied and the Cu assumes a fully symmetric tetrahedral configuration, with Cu—Si bond lengths of 2.240 Å. Removing one electron from $\text{Cu}_{\text{Si}}^{3-}$, the partial occupancy of the $t_2^{(p)}$ state drives a Jahn-Teller

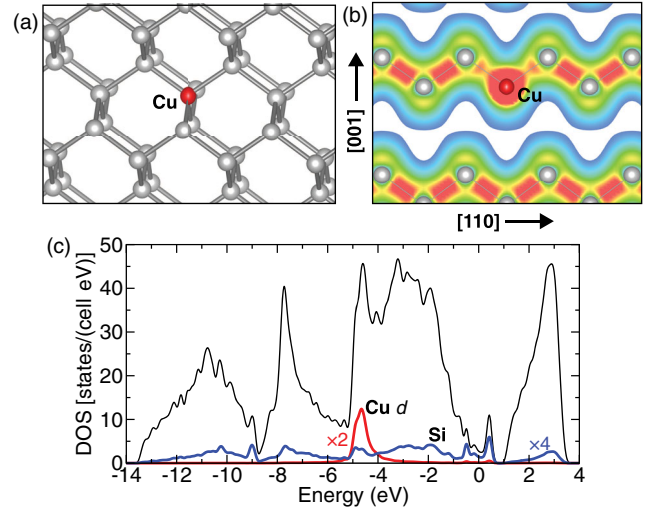


FIG. 5. (a) Ball-and-stick model of the local lattice structure of substitutional Cu in Si in the neutral charge state (Cu_{Si}^0). (b) Iso-surfaces of the total valence charge distribution of Cu_{Si}^0 in a (110) plane containing the Cu impurity and one of the nearest-neighbor Si atoms. (c) Total density of states (DOS) of a supercell containing Cu_{Si}^0 and the projections on the Cu and four nearest-neighbor Si sites showing the 3d contribution to the resonant states in the valence band and the Si contribution to the gap states.

distortion, lowering the symmetry to D_{2d} , and gives a net spin $S = 1/2$; the Cu impurity is slightly displaced along the [100] direction, by 0.030 Å, resulting in two sets of Cu—Si bond lengths of 2.270 and 2.280 Å. We test the

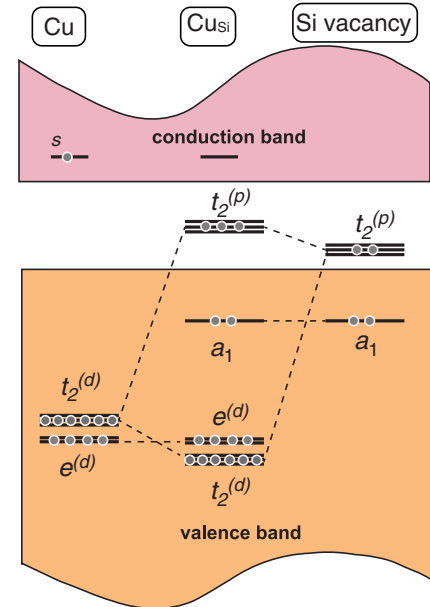


FIG. 6. Illustration of the origin of the defect-related states in the band gap for Cu_{Si} in the neutral charge state. The Cu d -related states are resonant in the valence band ($t_2^{(d)}$ and $e^{(d)}$), while the $t_2^{(p)}$ gap states originate mainly from the nearest-neighbor Si orbitals, i.e., the vacancy-related states.

displacement of the Cu impurity along the $[111]$ direction but find it 0.04 eV higher in energy than the $[100]$ displacement. The distortion results in a splitting of the $t_2^{(p)}$ state in a fully occupied twofold-degenerate state, and a spin-split onefold state, the highest of which is unoccupied. In the $\text{Cu}_{\text{Si}}^{-1}$ charge state, we find that the lowest energy configuration has $S = 0$ and a D_{2d} symmetry, with two Cu—Si bond lengths of 2.305 Å, and the other two of 2.31 Å.

In the neutral charge state Cu_{Si}^0 , the defect prefers a trigonal symmetry, C_{3v} , with three Cu—Si bond lengths of 2.335 Å, and one slightly longer Cu—Si bond of 2.348 Å, with $S = 1/2$. A high-spin $S = 3/2$ configuration, with tetrahedral symmetry, is only 0.013 eV higher in energy. Finally, in the positive charge state Cu_{Si}^+ , we find that the defect also prefers a trigonal configuration with $S = 0$, with three Cu—Si bond lengths of 2.372 Å and a slightly longer Cu—Si bond of 2.373 Å. The high-spin $S = 1$ configuration is higher in energy by 0.18 eV.

C. Cu_{Si} -Cu_i pair

Because of the high formation energies and low migration barrier, it is anticipated that interstitial Cu forms complexes with other defects in Si, including Cu_{Si} . From the results for Cu_i and Cu_{Si} discussed above, we expect that Cu_{Si} -Cu_i pairs are easier to form in *n*-type material since, in this case, the two defects have opposite charges, i.e., $\text{Cu}_{\text{Si}}^{-2}$ and Cu_{Si}^+ . The trapping of Cu_i^+ by $\text{Cu}_{\text{Si}}^{-2}$ explains the observed decrease of Cu diffusivity in *n*-type material [37] and also why Cu precipitates are easier to form in *n*-type than in *p*-type Si [37]. It also indicates that the binding energy of Cu_i and Cu_{Si} depends on the Fermi-level position.

The formation energy of the Cu_{Si} -Cu_i pair is shown Fig. 3(c). Similar to isolated Cu_{Si} , we find three transition levels for Cu_{Si} -Cu_i: a donor level (+/0) at 0.18 eV, an acceptor level (0/−) at 0.63 eV, and a double-acceptor level at 1.00 eV above the valence band. In this complex, Cu_i occupies a tetrahedral interstitial site next to Cu_{Si} , in a C_{3v} symmetry. Cu_{Si} is surrounded by four Si atoms and Cu_i, as shown in Fig. 7(a). In all charge states, we find one shorter Cu_{Si} —Si bond along the $[111]$ direction and three other longer Cu_{Si} —Si bonds. The Cu_{Si} —Cu_i bond length falls in between, except in the −2 charge state, where the Cu_{Si} —Cu_i bond is longer than all four Cu_{Si} —Si bonds. For example, in the neutral charge state, the Cu_{Si} —Si bond along the $[111]$ direction has a length of 2.242 Å, and the other three Cu_{Si} —Si bonds have a length equal to 2.378 Å, while the Cu_{Si} —Cu_i distance is 2.349 Å.

The electronic structure and transition levels of the Cu_{Si} -Cu_i complex is similar to those of isolated Cu_{Si} . The interstitial Cu in the complex does not induce gap states, and only provides an electron to the Cu_{Si} -related partially occupied states in the gap. In the −2 charge state of

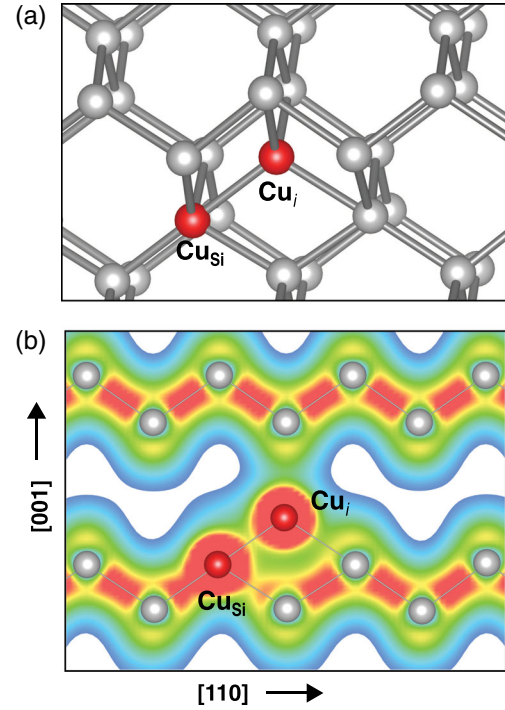


FIG. 7. (a) Ball-and-stick model of the local lattice structure of the Cu_{Si} -Cu_i pair in Si in the neutral charge state $[(\text{Cu}_{\text{Si}}-\text{Cu}_i)^0]$. (b) Isosurfaces of the total valence charge distribution of $(\text{Cu}_{\text{Si}}-\text{Cu}_i)^0$ in a (110) plane containing a Cu_{Si} -Cu_i pair.

the complex, all of the gap states are filled, and the complex can be considered composed of $\text{Cu}_{\text{Si}}^{-3}$ stabilized in the presence of Cu_i^+ . In fact, we can see that the bond between Cu_{Si} and Cu_i is significantly less covalent than the Cu_{Si} —Si and Si—Si bonds, as shown in the total valence charge distribution in Fig. 7(b).

The binding energy of Cu_{Si} -Cu_i is charge-state dependent and, therefore, depends on the position of the Fermi level in the gap. For instance, in *p*-type material, we find that the binding energy of $(\text{Cu}_{\text{Si}}-\text{Cu}_i)^+$ with respect to isolated Cu_{Si}^0 and Cu_i^+ amounts to 0.77 eV. Adding the migration barrier of 0.19 eV for Cu_i^+ , the estimated dissociation energy amounts to 0.96 eV. If the Fermi level falls between the (+/0) and (0/−) levels, the binding energy of $(\text{Cu}_{\text{Si}}-\text{Cu}_i)^0$ with respect to isolated Cu_{Si}^- and Cu_i^+ is 1.13 eV. This result is larger than the value of 0.78 eV reported in a previous study [55], yet consistent with a stronger attractive interaction between Cu_{Si}^- and Cu_i^+ than between Cu_{Si}^0 and Cu_i^+ . If the Fermi level falls in the upper part of the band gap, between the (0/−) and (−/−2) levels, the binding energy of $(\text{Cu}_{\text{Si}}-\text{Cu}_i)^-$ with respect to isolated $\text{Cu}_{\text{Si}}^{-2}$ and Cu_i^+ is 1.47 eV. Finally, in *n*-type material, to separate $(\text{Cu}_{\text{Si}}-\text{Cu}_i)^{-2}$ into $\text{Cu}_{\text{Si}}^{-2}$ and Cu_i^+ requires an energy of 1.64 eV plus the release of one electron in the conduction band. We note that the prevalence of Cu_{Si} -Cu_i in a negative charge state in *n*-type Si

makes it more likely to attract Cu_i^+ , favoring the formation of complexes with more than two Cu atoms, and explains why Cu clustering is most favorable in *n*-type material [37]. It is known that Cu complexes including four Cu atoms exist and are believed to be the reason behind intense photoluminescence (PL) emission with a zero-phonon line at 1014 meV [79,80], referred to as a Cu_{PL} line. We discuss the results for the complex containing four Cu atoms, formed by a substitutional Cu and three neighboring interstitial Cu ($\text{Cu}_{\text{Si}}\text{-}3\text{Cu}_i$) atoms below.

D. $\text{Cu}_{\text{Si}}\text{-H}_i$ complex

Hydrogen is a ubiquitous impurity in semiconductors which can be incorporated through implantation, plasma annealing, or chemical wetting [81,82]. It can also be unintentionally incorporated from a metal contact, a surface layer, or organic masks. In silicon, H occupies interstitial sites and rapidly diffuses through the material. It strongly interacts with impurities and native defects, affecting their behavior in most cases. Hydrogen is amphoteric, being able to passivate or compensate for acceptors and donors, counteracting the prevailing conductivity [81]. In particular, H forms strong bonds with transition-metal impurities, including Cu [83].

Experiments indicate that Cu_{Si} can form complexes with more than one H atom [33,36,40]. DLTS spectra of $\text{Cu}_{\text{Si}}\text{-H}_i$ and $\text{Cu}_{\text{Si}}\text{-}2\text{H}_i$ have been reported. Here, we limit our study to the complex involving Cu_{Si} and one H atom. The calculated formation energy as a function of the Fermi-level position for the $\text{Cu}_{\text{Si}}\text{-H}_i$ pair [Fig. 3(d)] shows three transition levels in the gap: a donor level (+/0) at 0.04 eV, an acceptor level (0/−) at 0.44 eV, and a double-acceptor level (−/−2) at 0.85 eV above the valence band. For comparison, recent experimental results based on Laplace-transform DLTS reveal two levels associated with $\text{Cu}_{\text{Si}}\text{-H}_i$, (+/0) at 0.10 eV and (0/−) at 0.49 eV above the valence band [40]. A previous DLTS measurement indicates that there is a double-acceptor (−/−2) level at 0.81 eV above the valence band [36]. The level structure is similar to that of isolated Cu_{Si} and the $\text{Cu}_{\text{Si}}\text{-Cu}_i$ pair, and it suggests that H_i provides an electron to occupy the Cu_{Si} -related $t_2^{(p)}$ gap states.

We find that H prefers to bind to Cu_{Si} forming a bond along the [001] direction, as shown in Fig. 8(a), in all four charge states. In the neutral charge state, the $\text{Cu}_{\text{Si}}\text{-H}_i$ bond length is 1.557 Å, and the distance between H_i and the two nearby Si atoms is 1.932 Å. The $\text{Cu}_{\text{Si}}\text{-H}_i$ and $\text{H}_i\text{-Si}$ distances slightly decrease, by about 0.03 Å, going from the +1 to the −2 charge state. From the valence charge distribution shown in Fig. 8(b), we can see a strong bond between Cu_{Si} and H_i , with a much weaker yet noticeable interaction between H_i and the neighboring Si atoms.

We also calculate the binding energy for the $\text{Cu}_{\text{Si}}\text{-H}_i$ pair, i.e., to break the pair into isolated Cu_{Si} and H_i atoms. Our calculations for the isolated H_i atom show that only the

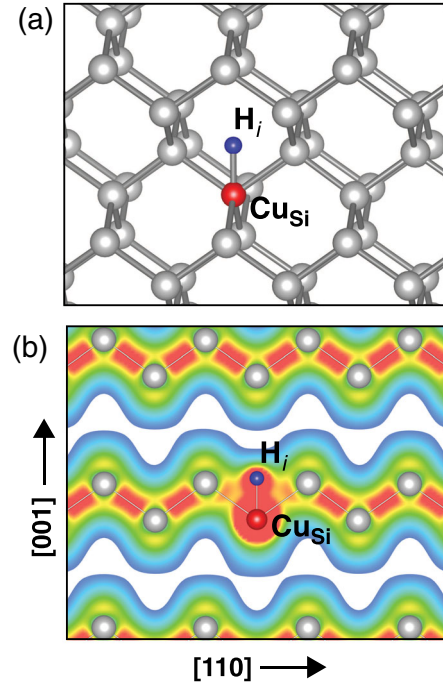


FIG. 8. (a) Ball-and-stick model of the local lattice structure of the $\text{Cu}_{\text{Si}}\text{-H}_i$ complex in Si, in the neutral charge state $[(\text{Cu}_{\text{Si}}\text{-H}_i)^0]$. (b) Isosurfaces of the total valence charge distribution of $(\text{Cu}_{\text{Si}}\text{-H}_i)^0$ in a (110) plane containing Cu_{Si} and H_i .

single-donor and -acceptor charge states are stable for Fermi-level positions in the gap, forming a negative-*U* center, in agreement with previous studies [81]. The (+/−) transition level occurs at 0.83 eV above the valence band. In the donor charge state, H_i prefers a bond-center configuration, with two equal $\text{H}_i\text{-Si}$ bond lengths of 1.576 Å. On the other hand, in the acceptor charge state, it prefers the antibonding site (along the [111] direction) with a Si—H bond length of 1.730 Å.

In *p*-type doped material, with a Fermi level at or near the VBM, the binding energy of $(\text{Cu}_{\text{Si}}\text{-H}_i)^+$ with respect to $\text{Cu}_{\text{Si}}^0 + \text{H}_i^+$ amounts to 0.84 eV. We note that, despite the positive binding energy—i.e., a situation where the pair is more stable than the isolated species—the $(\text{Cu}_{\text{Si}}\text{-H}_i)^+$ complex has a low probability of forming in *p*-type material due to the Coulomb repulsion between Cu_{Si}^+ and H_i^+ . This result may explain the difficulties in the identification of (+/0) level [36]. For a Fermi level between (+/0) and (0/−), i.e., in the range 0.04–0.44 eV, the binding energy of $(\text{Cu}_{\text{Si}}\text{-H}_i)^0$ with respect to isolated Cu_{Si} and H_i^+ atoms is 1.35 eV. If the Fermi level falls between (0/−) and (−/−2), the binding energy of $(\text{Cu}_{\text{Si}}\text{-H}_i)^-$ with respect to $\text{Cu}_{\text{Si}}^{+2}$ and H_i^+ is 1.88 eV, and, for a Fermi level in a narrow range in the upper part of the band gap—between 0.85 and 0.97 eV—the energy to separate $(\text{Cu}_{\text{Si}}\text{-H}_i)^{-2}$ into Cu_{Si}^- and H_i^- is 1.72 eV. For a Fermi level above 0.97 eV, i.e., above the (−/−2) level of Cu_{Si} , or in *n*-type material,

breaking $(\text{Cu}_{\text{Si}}\text{-H}_i)^{-2}$ into $\text{Cu}_{\text{Si}}^{-2}$ and H_i^- requires the capture of one electron from the conduction band and costs 1.53 eV. We note that the formation of $(\text{Cu}_{\text{Si}}\text{-H}_i)^{-2}$ will occur with a low probability due to the Coulomb repulsion between $\text{Cu}_{\text{Si}}^{-2}$ and H_i^- in n -type material. These results are somewhat smaller than the value of 2.3 eV reported in a previous theoretical study since the authors considered neutral interstitial H a product of the reaction [83].

E. $\text{Cu}_{\text{Si}}\text{-3Cu}_i$ complex

Photoluminescence studies of Cu-related complexes in silicon have shown an intense zero-phonon line at 1.014 eV [84] and a related donor level at 0.10 eV above the valence band by DLTS measurements [21,22]. It was concluded that the 1.014 eV line is associated with a complex composed of at least four Cu atoms with trigonal symmetry, referred to as the Cu_{PL} center [80]. Based on DFT calculations, Shirai *et al.* [79] proposed that a complex composed of Cu_{Si} and three neighboring Cu_i atoms with a trigonal symmetry ($\text{Cu}_{\text{Si}}\text{-3Cu}_i$) as responsible for the 1.014-eV line. Subsequent DFT calculations by Carvalho *et al.* [55] showed that the $\text{Cu}_{\text{Si}}\text{-3Cu}_i$ complex is indeed the lowest energy configuration among the possible complexes involving four Cu impurities. The calculations by Carvalho *et al.* predicted a $(+/-0)$ donor level 0.25 eV above the valence band, and the authors suggested that this complex could explain the level 0.10 eV observed in the DLTS measurements [21,22]. Considering the band-gap error in these earlier calculations, it is hard to justify the discrepancy between the theoretical and experimental values.

Using the HSE06 functional and a 216-atom supercell, we also carry out calculations for the $\text{Cu}_{\text{Si}}\text{-3Cu}_i$ complex. The calculated formation energies are shown in Fig. 3(e), and the relaxed local lattice configuration is shown in Fig. 9(a). We find two levels in the gap, a $(+2/+)$ level at 0.26 eV and a $(+/-0)$ level at 0.37 eV above the valence band. By comparison, Carvalho *et al.* [55] reported only a $(+/-0)$ level at 0.25 eV. We attribute this difference to the band-gap error in the previous calculations. We note that the single-donor level at 0.37 eV is too far from the observed level at 0.10 eV assigned to the Cu_{PL} defect [21,22].

$\text{Cu}_{\text{Si}}\text{-3Cu}_i$ in the neutral charge state corresponds to each Cu_i giving away one electron to fill the levels associated with Cu_{Si} , resulting in all levels in the gap being filled. The charge-density distribution of $\text{Cu}_{\text{Si}}\text{-3Cu}_i$ in the (110) plane passing through Cu_{Si} and one of the neighboring Cu_i atoms is shown in Fig. 9(b), demonstrating the similarities between the $\text{Cu}_{\text{Si}}\text{-3Cu}_i$ and the $\text{Cu}_{\text{Si}}\text{-Cu}_i$ complex in Fig. 7(b). While the thermodynamic transition levels $(+2/+)$ and $(+/-0)$ are located in the lower part of the gap, the filled single-particle states are at 0.7 eV (onfold degenerate) and 0.6 eV (twofold degenerate) above the valence band. Based on these single-particle levels in the gap, we estimate an optical-emission-energy

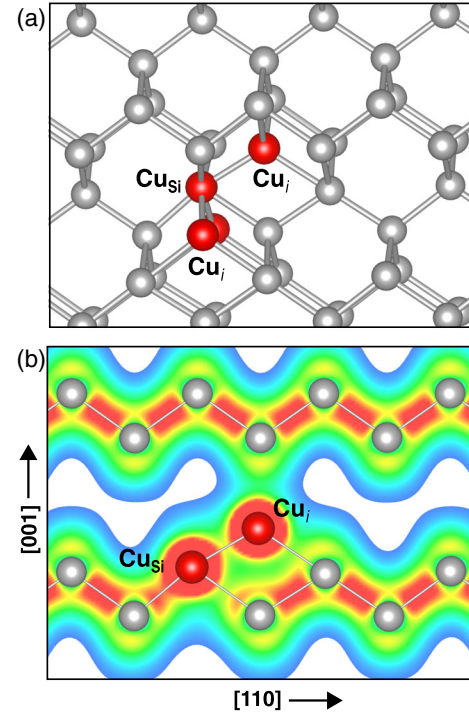


FIG. 9. (a) Ball-and-stick model of the local lattice structure of the $\text{Cu}_{\text{Si}}\text{-3Cu}_i$ complex in the neutral charge state $[(\text{Cu}_{\text{Si}}\text{-3Cu}_i)^0]$. (b) Isosurface of the total valence charge distribution of $(\text{Cu}_{\text{Si}}\text{-3Cu}_i)^0$ in a (110) plane containing Cu_{Si} and one Cu_i atom.

peak at about 0.5 eV, which is much smaller than the observed 1.014-eV line for the Cu_{PL} center [80].

Based on our results, we can rule out $\text{Cu}_{\text{Si}}\text{-3Cu}_i$ being responsible for the transition level at 0.10 eV by DLTS measurements [21,22] and the peak at 1.014 eV observed in photoluminescence experiments [80,84].

Recent experiments based on infrared spectroscopy and photoconductivity measurements indicated the existence of a shallow acceptor $(0/-)$ level, with an ionization energy of 27 meV, associated with the Cu impurity in Si [42]. We note that none of the centers studied in the

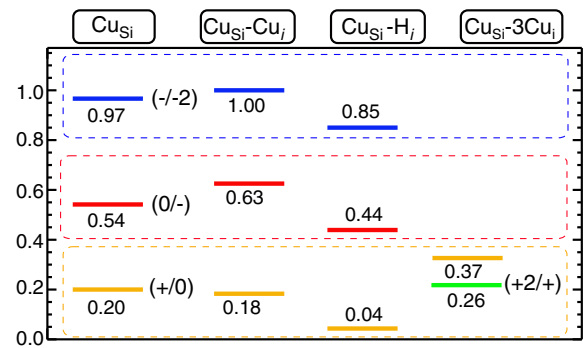


FIG. 10. Calculated transition levels for the substitutional Cu_{Si} atom, the $\text{Cu}_{\text{Si}}\text{-Cu}_i$ pair, the copper-hydrogen pair $\text{Cu}_{\text{Si}}\text{-H}_i$, and the $\text{Cu}_{\text{Si}}\text{-3Cu}_i$ complex. The zero in energy is placed at the VBM.

present work can explain this shallow acceptor level. It was then proposed that the shallow acceptor ($0/-$) level would universally align in an absolute energy scale when the band offsets between the various semiconductors were taken into account [42]. Given that the gap levels of Cu_{Si} are associated with $t_2^{(p)}$ states, which are derived mostly from orbitals of the host atoms, we would not expect these levels to follow a universal alignment, but rather that they would be strongly dependent on the host material. Therefore, our results cannot explain the Cu-related shallow acceptor level observed in Ref. [42], for which further calculations of complexes and experiments are needed for a full characterization. These complexes could perhaps involve interstitial Cu trapped by an acceptor impurity.

Finally, our results indicate that Cu_{Si} and related complexes induce gap states, as summarized in Fig. 10, and that, if these defects are present in sufficient concentrations, they can cause leakage current, increasing the tunneling probability of electrons from filled impurity-induced states to empty states in the conduction band in Si devices. Note that the Cu-related defects are not the only or even the main source of leakage current observed in Si devices since their concentrations are relatively low in most devices that do not use copper as contacts [2–5]. The different behavior of Cu in p -Si and n -Si, as suggested previously [12,15], can be attributed to the fact that Cu_i is stable in the $+1$ charge state and tends to form complexes, such as $\text{Cu}_{\text{Si}}\text{-Cu}_i$ and $\text{Cu}_{\text{Si}}\text{-H}_i$, that are more stable in n -Si than in p -Si and $\text{Cu}_{\text{Si}}\text{-3Cu}_i$ which is more stable in p -Si than in n -Si. On the other hand, the complexes involving Cu_i and shallow acceptors are expected to be electrically inactive with no levels in the gap and, hence, will not affect the minority-carrier lifetime.

IV. SUMMARY AND CONCLUSIONS

Using the HSE06 hybrid functional, we calculate in this paper formation energies and transition levels for interstitial Cu_i , substitutional Cu_{Si} , the $\text{Cu}_{\text{Si}}\text{-Cu}_i$ pair, $\text{Cu}_{\text{Si}}\text{-H}_i$, and the $\text{Cu}_{\text{Si}}\text{-3Cu}_i$ complex in Si. We find that Cu_i is a shallow donor and a fast diffuser with a calculated migration barrier of only 0.19 eV. Substitutional Cu_{Si} , the $\text{Cu}_{\text{Si}}\text{-Cu}_i$ pair, and the $\text{Cu}_{\text{Si}}\text{-H}_i$ complex all induce donor and acceptor levels in the gap, while the $\text{Cu}_{\text{Si}}\text{-3Cu}_i$ complex induces two donor levels in the gap. The level structures of the $\text{Cu}_{\text{Si}}\text{-Cu}_i$ pair, $\text{Cu}_{\text{Si}}\text{-H}_i$, and the $\text{Cu}_{\text{Si}}\text{-3Cu}_i$ complexes are derived from that of Cu_{Si} , meaning that levels reflect the occupancy of ligand-derived $t_2^{(p)}$ states in the band gap, while the Cu-related $t_2^{(d)}$ states are resonant in the valence band, about 5 eV below the VBM. The present calculations show a significant improvement over previous theoretical studies when compared to the available experimental data, providing a quantitative description of the position of the transition levels in the band gap.

ACKNOWLEDGMENTS

A. S. and A. J. acknowledge the financial support from the U.S. Department of Energy under Grant No. DE-SC0014388. This work used the Extreme Science and Engineering Discovery Environment (XSEDE), which is supported by National Science Foundation Grant No. ACI-1053575, and was also supported in part through the use of Information Technologies (IT) resources at the University of Delaware, specifically the high-performance computing resources.

-
- [1] K. Graff, *Metal Impurities in Silicon-Device Fabrication*, Springer Series in Materials Science Vol. 24 (Springer, Berlin, 1995), p. 143.
 - [2] A. Goetzberger and W. Shockley, Metal precipitates in silicon p - n junctions, *J. Appl. Phys.* **31**, 1821 (1960).
 - [3] H. H. Busta and H. A. Waggener, Precipitation-induced currents and generation-recombination currents in intentionally contaminated silicon P^+N junctions, *J. Electrochem. Soc.* **124**, 1424 (1977).
 - [4] R. Böhm and H. Klose, Copper in silicon $n^+ - p$ junctions, *Phys. Status Solidi (a)* **9**, K165 (1972).
 - [5] R. Hamaker, Z. Putney, R. Ayers, and P. Smith, Degradation mechanism for silicon $p^+ - n$ junctions under forward bias, *Solid State Electron.* **24**, 1001 (1981).
 - [6] K. Honda, A. Ohsawa, and N. Toyokura, Breakdown in silicon oxides correlation with Cu precipitates, *Appl. Phys. Lett.* **45**, 270 (1984).
 - [7] K. Hiramoto, M. Sano, S. Sadamitsu, and N. Fujino, Degradation of gate oxide integrity by metal impurities, *Jpn. J. Appl. Phys.* **28**, L2109 (1989).
 - [8] M. Datta, Applications of electrochemical microfabrication: An introduction, *IBM J. Res. Dev.* **42**, 563 (1998).
 - [9] J. R. Davis, A. Rohatgi, R. H. Hopkins, P. D. Blais, P. Rai-Choudhury, J. R. McCormick, and H. C. Mollenkopf, Impurities in silicon solar cells, *IEEE Trans. Electron Devices* **27**, 677 (1980).
 - [10] R. Hopkins and A. Rohatgi, Impurity effects in silicon for high efficiency solar cells, *J. Cryst. Growth* **75**, 67 (1986).
 - [11] H. Prigge, P. Gerlach, P. O. Hahn, A. Schnegg, and H. Jacob, Acceptor compensation in silicon induced by chemomechanical polishing, *J. Electrochem. Soc.* **138**, 1385 (1991).
 - [12] S. Naito and T. Nakashizu, Electric degradation and defect formation of silicon due to Cu, Fe, and Ni contamination, *MRS Online Proc. Libr.* **262**, 641 (1992).
 - [13] M. Itsumi, Y. Sato, K. Imai, and N. Yabumoto, Characterization of metallic impurities in Si using a recombination-lifetime correlation method, *J. Appl. Phys.* **82**, 3250 (1997).
 - [14] A. L. P. Rotondaro, T. Q. Hurd, A. Kaniava, J. Vanhellemont, E. Simoen, M. M. Heyns, C. Claeys, and G. Brown, Impact of Fe and Cu contamination on the minority carrier lifetime of silicon substrates, *J. Electrochem. Soc.* **143**, 3014 (1996).
 - [15] W. B. Henley, D. A. Ramappa, and L. Jastrzebski, Detection of copper contamination in silicon by surface photovoltage diffusion length measurements, *Appl. Phys. Lett.* **74**, 278 (1999).

- [16] J. Steigman, W. Shockley, and F. C. Nix, The self-diffusion of copper, *Phys. Rev.* **56**, 13 (1939).
- [17] C. B. Collins and R. O. Carlson, Properties of silicon doped with iron or copper, *Phys. Rev.* **108**, 1409 (1957).
- [18] R. N. Hall and J. H. Racette, Diffusion and solubility of copper in extrinsic and intrinsic germanium, silicon, and gallium arsenide, *J. Appl. Phys.* **35**, 379 (1964).
- [19] E. R. Weber, Transition metals in silicon, *Appl. Phys. A* **30**, 1 (1983).
- [20] A. J. Tavendale and S. J. Pearton, Deep level, quenched-in defects in silicon doped with gold, silver, iron, copper or nickel, *J. Phys. C* **16**, 1665 (1983).
- [21] H. Lemke, Interference reactions in Cu-doped silicon crystals, *Phys. Status Solidi (a)* **95**, 665 (1986).
- [22] S. D. Brotherton, J. R. Ayres, A. Gill, H. W. Van Kesteren, and F. J. A. M. Greidanus, Deep levels of copper in silicon, *J. Appl. Phys.* **62**, 1826 (1987).
- [23] A. A. Istratov, H. Hieslmair, C. Flink, T. Heiser, and E. R. Weber, Interstitial copper-related center in *n*-type silicon, *Appl. Phys. Lett.* **71**, 2349 (1997).
- [24] A. A. Istratov, C. Flink, H. Hieslmair, E. R. Weber, and T. Heiser, Intrinsic Diffusion Coefficient of Interstitial Copper in Silicon, *Phys. Rev. Lett.* **81**, 1243 (1998).
- [25] A. A. Istratov and E. R. Weber, Electrical properties and recombination activity of copper, nickel and cobalt in silicon, *Appl. Phys. A* **66**, 123 (1998).
- [26] A. A. Istratov, H. Hieslmair, T. Heiser, C. Flink, and E. R. Weber, The dissociation energy and the charge state of a copper-pair center in silicon, *Appl. Phys. Lett.* **72**, 474 (1998).
- [27] M. Nakamura, Dissociation of the 1.014 eV photoluminescence copper center in silicon crystal, *Appl. Phys. Lett.* **73**, 3896 (1998).
- [28] T. Heiser, A. A. Istratov, C. Flink, and E. R. Weber, Electrical characterization of copper related defect reactions in silicon, *Mater. Sci. Eng. B* **58**, 149 (1999).
- [29] C. Flink, H. Feick, S. A. McHugo, A. Mohammed, W. Seifert, H. Hieslmair, T. Heiser, A. A. Istratov, and E. R. Weber, Formation of copper precipitates in silicon, *Physica (Amsterdam)* **273B–274B**, 437 (1999).
- [30] S. Knack, J. Weber, and H. Lemke, Copper-hydrogen complexes in silicon, *Physica (Amsterdam)* **274B**, 387 (1999).
- [31] U. Wahl, A. Vantomme, G. Langouche, and J. G. Correia (for the ISOLDE Collaboration), Lattice Location and Stability of Ion Implanted Cu in Si, *Phys. Rev. Lett.* **84**, 1495 (2000).
- [32] U. Wahl, A. Vantomme, G. Langouche, J. P. Arajo, L. Peralta, and J. G. Correia, Lattice location of implanted Cu in highly doped Si, *Appl. Phys. Lett.* **77**, 2142 (2000).
- [33] S. Knack, J. Weber, H. Lemke, and H. Riemann, Copper-hydrogen complexes in silicon, *Phys. Rev. B* **65**, 165203 (2002).
- [34] A. A. Istratov and E. R. Weber, Physics of copper in silicon, *J. Electrochem. Soc.* **149**, G21 (2002).
- [35] T. Heiser, A. Belayachi, and J. P. Schunck, Copper behavior in bulk silicon and associated characterization techniques, *J. Electrochem. Soc.* **150**, G831 (2003).
- [36] S. Knack, Copper-related defects in silicon, *Mater. Sci. Semicond. Process.* **7**, 125 (2004).
- [37] H. Bracht, Copper related diffusion phenomena in germanium and silicon, *Mater. Sci. Semicond. Process.* **7**, 113 (2004).
- [38] M. Nakamura and S. Murakami, Deep-level transient spectroscopy and photoluminescence studies of formation and depth profiles of copper centers in silicon crystals diffused with dilute copper, *Jpn. J. Appl. Phys.* **49**, 713021 (2010).
- [39] M. Nakamura, S. Murakami, and H. Uono, Energy level(s) of the dissociation product of the 1.014 eV photoluminescence copper center in *n*-type silicon determined by photoluminescence and deep-level transient spectroscopy, *J. Appl. Phys.* **114**, 033508 (2013).
- [40] N. Yarykin and J. Weber, Deep levels of copper-hydrogen complexes in silicon, *Phys. Rev. B* **88**, 085205 (2013).
- [41] N. A. Yarykin and J. Weber, Identification of copper-copper and copper-hydrogen complexes in silicon, *Semiconductors* **47**, 275 (2013).
- [42] S. T. Teklemichael, M. D. McCluskey, G. Buchowicz, O. D. Dubon, and E. E. Haller, Evidence for a shallow Cu acceptor in Si from infrared spectroscopy and photoconductivity, *Phys. Rev. B* **90**, 165204 (2014).
- [43] A. Zunger and U. Lindefelt, Theory of substitutional and interstitial *3d* impurities in silicon, *Phys. Rev. B* **26**, 5989 (1982).
- [44] A. Fazzio, M. J. Caldas, and A. Zunger, Electronic structure of copper, silver, and gold impurities in silicon, *Phys. Rev. B* **32**, 934 (1985).
- [45] C. Delerue, M. Lannoo, and G. Allan, New theoretical approach of transition-metal impurities in semiconductors, *Phys. Rev. B* **39**, 1669 (1989).
- [46] S. K. Estreicher, Copper, lithium, and hydrogen passivation of boron in *c*-Si, *Phys. Rev. B* **41**, 5447 (1990).
- [47] F. Beeler, O. Andersen, and M. Scheffler, Electronic and magnetic structure of *3d* transition-metal point defects in silicon calculated from first principles, *Phys. Rev. B* **41**, 1603 (1990).
- [48] S. Estreicher, Rich chemistry of copper in crystalline silicon, *Phys. Rev. B* **60**, 5375 (1999).
- [49] S. K. Estreicher, First-principles theory of copper in silicon, *Mater. Sci. Semicond. Process.* **7**, 101 (2004).
- [50] C. D. Latham, M. Alatalo, R. M. Nieminen, R. Jones, S. Öberg, and P. R. Briddon, Passivation of copper in silicon by hydrogen, *Phys. Rev. B* **72**, 235205 (2005).
- [51] F. J. H. Ehlers, A. P. Horsfield, and D. R. Bowler, Electronic state of interstitial Cu in bulk Si: Density functional calculations, *Phys. Rev. B* **73**, 165207 (2006).
- [52] C. D. Latham, M. Ganchenkova, R. M. Nieminen, S. Nicolaysen, M. Alatalo, S. Öberg, and P. R. Briddon, Electronic structure calculations for substitutional copper and monovacancies in silicon, *Phys. Scr.* **T126**, 61 (2006).
- [53] K. Matsukawa, K. Shirai, H. Yamaguchi, and H. Katayama-Yoshida, Diffusion of transition-metal impurities in silicon, *Physica (Amsterdam)* **401B–402B**, 151 (2007).
- [54] H. Yamaguchi, K. Shirai, and H. Katayama-Yoshida, The stable site and diffusion of impurity Cu in Si, *J. Comput. Theor. Nanosci.* **6**, 2619 (2009).
- [55] A. Carvalho, D. J. Backlund, and S. K. Estreicher, Four-copper complexes in Si and the Cu-photoluminescence

- defect: A first-principles study, *Phys. Rev. B* **84**, 155322 (2011).
- [56] R. W. Godby, M. Schlüter, and L. J. Sham, Accurate Exchange-Correlation Potential for Silicon and Its Discontinuity on Addition of an Electron, *Phys. Rev. Lett.* **56**, 2415 (1986).
- [57] A. Seidl, A. Görling, P. Vogl, J. A. Majewski, and M. Levy, Generalized Kohn-Sham schemes and the band-gap problem, *Phys. Rev. B* **53**, 3764 (1996).
- [58] A. Janotti and C. G. Van de Walle, Native point defects in ZnO, *Phys. Rev. B* **76**, 165202 (2007).
- [59] J. Heyd, G. E. Scuseria, and M. Ernzerhof, Hybrid functionals based on a screened Coulomb potential, *J. Chem. Phys.* **118**, 8207 (2003).
- [60] J. Heyd, G. E. Scuseria, and M. Ernzerhof, Hybrid functionals based on a screened Coulomb potential, *J. Chem. Phys.* **118**, 8207 (2003); **124**, 219906(E) (2006).
- [61] J. L. Lyons, A. Janotti, and C. G. Van de Walle, Role of Si and Ge as impurities in ZnO, *Phys. Rev. B* **80**, 205113 (2009).
- [62] A. Janotti, J. L. Lyons, and C. G. Van de Walle, Hybrid functional calculations of native point defects in InN, *Phys. Status Solidi (a)* **209**, 65 (2012).
- [63] P. Hohenberg and W. Kohn, Inhomogeneous electron gas, *Phys. Rev.* **136**, B864 (1964).
- [64] W. Kohn and L. J. Sham, Self-consistent equations including exchange and correlation effects, *Phys. Rev.* **140**, A1133 (1965).
- [65] G. Kresse and J. Furthmüller, Efficient iterative schemes for ab initio total-energy calculations using a plane-wave basis set, *Phys. Rev. B* **54**, 11169 (1996).
- [66] G. Kresse and J. Furthmüller, Efficiency of ab initio total energy calculations for metals and semiconductors using a plane-wave basis set, *Comput. Mater. Sci.* **6**, 15 (1996).
- [67] J. P. Perdew, K. Burke, and M. Ernzerhof, Generalized Gradient Approximation Made Simple, *Phys. Rev. Lett.* **77**, 3865 (1996).
- [68] P. E. Blöchl, Projector augmented-wave method, *Phys. Rev. B* **50**, 17953 (1994).
- [69] G. Kresse and D. Joubert, From ultrasoft pseudopotentials to the projector augmented-wave method, *Phys. Rev. B* **59**, 1758 (1999).
- [70] W. M. Yim and R. J. Paff, Thermal expansion of AlN, sapphire, and silicon, *J. Appl. Phys.* **45**, 1456 (1974).
- [71] W. Bludau, A. Onton, and W. Heinke, Temperature dependence of the band gap of silicon, *J. Appl. Phys.* **45**, 1846 (1974).
- [72] C. Freysoldt, B. Grabowski, T. Hickel, J. Neugebauer, G. Kresse, A. Janotti, and C. G. Van de Walle, First-principles calculations for point defects in solids, *Rev. Mod. Phys.* **86**, 253 (2014).
- [73] H. H. Woodbury and G. W. Ludwig, Spin resonance of Pd and Pt in silicon, *Phys. Rev.* **126**, 466 (1962).
- [74] S. Kogan and K. B. Tolpygo, States of substitution impurity atoms of IB group elements in Si and Ge with 3 negative charges, *Fiz. Tverd. Tela (Leningrad)* **15**, 1544 (1973).
- [75] S. Kogan and K. B. Tolpygo, States of negative triply charged substitutional impurity atoms of group IB elements in Si and Ge, *Sov. Phys. Solid State* **15**, 1034 (1973).
- [76] S. Kogan and K. B. Tolpygo, Theory of deep impurity centers in silicon, *Fiz. Tverd. Tela (Leningrad)* **16**, 3176 (1974).
- [77] S. Kogan and K. B. Tolpygo, Theory of deep impurity centres in silicon, *Sov. Phys. Solid State* **16**, 2067 (1975).
- [78] D. E. Woon, D. S. Marynick, and S. K. Estreicher, Titanium and copper in Si: Barriers for diffusion and interactions with hydrogen, *Phys. Rev. B* **45**, 13383 (1992).
- [79] K. Shirai, H. Yamaguchi, A. Yanase, and H. Katayama-Yoshida, A new structure of Cu complex in Si and its photoluminescence, *J. Phys. Condens. Matter* **21**, 064249 (2009).
- [80] M. Steger, A. Yang, N. Stavrias, M. L. W. Thewalt, H. Riemann, N. V. Abrosimov, M. F. Churbanov, A. V. Gusev, A. D. Bulanov, I. D. Kovalev, A. K. Kaliteevskii, O. N. Godisov, P. Becker, and H. J. Pohl, Reduction of the Linewidths of Deep Luminescence Centers in ²⁸Si Reveals Fingerprints of the Isotope Constituents, *Phys. Rev. Lett.* **100**, 177402 (2008).
- [81] C. G. Van de Walle, P. J. H. Denteneer, Y. Bar-Yam, and S. T. Pantelides, Theory of hydrogen diffusion and reactions in crystalline silicon, *Phys. Rev. B* **39**, 10791 (1989).
- [82] S. M. Myers, M. I. Baskes, H. K. Birnbaum, J. W. Corbett, G. G. DeLeo, S. K. Estreicher, E. E. Haller, P. Jena, N. M. Johnson, R. Kirchheim, S. J. Pearton, and M. J. Stavola, Hydrogen interactions with defects in crystalline solids, *Rev. Mod. Phys.* **64**, 559 (1992).
- [83] D. West, S. K. Estreicher, S. Knack, and J. Weber, Copper interactions with H, O, and the self-interstitial in silicon, *Phys. Rev. B* **68**, 035210 (2003).
- [84] J. Weber, H. Bauch, and R. Sauer, Optical properties of copper in silicon: Excitons bound to isoelectronic copper pairs, *Phys. Rev. B* **25**, 7688 (1982).